ISSN: 2447-3359

REVISTA DE GEOCIÊNCIAS DO NORDESTE

Northeast Geosciences Journal

v. 11, nº 1 (2025)

https://doi.org/10.21680/2447-3359.2025v11n1ID38938

Mining Tailings Dam Monitoring Using Geophysical Methods: Ambient Noise Seismic Interferometry and Electrical Resistivity – B1B4 Dam, Araxá (MG)

Monitoramento de Barragem de Rejeito Através de Métodos Geofísicos: Interferometria Sísmica do Ruído Ambiente e Eletrorresistividade – Barragem B1B4, Araxá (MG)

Anne Karine Nunes da Mata Silva[1]; Marco Antonio da Silva Braga[2]; Maria Filipa Perez da Gama[3] ; Gilvan Sá[4]; Ewerton Aparecido Rodrigues[5]; Igor Leonardo Gama[6]; Thiago Oliveira[7]; Ricardo Luiz Teixeira Telles[8]

[1] Federal University of Rio de Janeiro, Applied Geophysics Research Center (CPGA)/ Geology Department, Rio de Janeiro/RJ, Brazil. Email: annekarine@geologia.ufrj.br
ORCID: https://orcid.org/0009-0002-8166-1435

[2] Federal University of Rio de Janeiro, Applied Geophysics Research Center (CPGA)/ Geology Department, Rio de Janeiro/RJ, Brazil. Email: marcobraga@geologia.ufrj.br
ORCID: https://orcid.org/0000-0002-0244-4655

[3] Federal University of Rio de Janeiro, Applied Geophysics Research Center (CPGA)/ Geology Department, Rio de Janeiro/RJ, Brazil.. Email: filipa@geologia.ufrj.br
ORCID: https://orcid.org/0000-0002-8084-8954

[4] Federal University of Ouro Preto, Ouro Preto/MG, Brazil. Email: gilvansa1972@gmail.com
ORCID: https://orcid.org/0000-0001-7303-0778

[5] Mosaic Fertilizantes do Brasil, Araxá/MG, Brazil. Email: ewerton.rodrigues@mosaicco.com
ORCID: https://orcid.org/0009-0008-2854-5615

[6] Mosaic Fertilizantes do Brazil, Araxá/MG, Brasil. Email: igor.gama2@mosaicco.com
ORCID: https://orcid.org/0009-0005-3069-5709

[7] Mosaic Fertilizantes do Brazil, Araxá/MG, Brasil. Email: thiago.oliveira20@mosaicco.com
ORCID: https://orcid.org/0009-0004-5603-5517

[8] Mosaic Fertilizantes do Brazil, Araxá/MG, Brasil. Email: ricardo.telles@mosaicco.com
ORCID: https://orcid.org/0009-0007-2287-8120

Abstract: Tailings dams for mining and industrial waste require constant monitoring due to their environmental impact and the risk of failure. In Brazil, there are 941 registered dams, 340 of which are located in Minas Gerais. To ensure the integrity of these structures, monitoring is conducted through visual inspections and conventional instrumentation, such as piezometers, which require significant time and planning for data processing. Geophysical methods emerge as complementary alternatives, offering broader coverage and faster data acquisition. Thus, this study aims to evaluate the physical parameters of the B1B4 Dam, located in Araxá, using Ambient Noise Seismic Interferometry, which monitors variations in the S-wave velocity (Vs), enabling the assessment of changes in the structure's stiffness modulus, and electrical resistivity, which identifies moisture zones categorized into low (<56 ohm.m), intermediate, and high resistivity zones (>371 ohm.m). Seismic interferometry data showed greater variations in Vs during periods of high rainfall, suggesting changes in the physical properties of the dam body. Electrical resistivity data indicated the presence of conductive and resistive areas, providing information to identify "Higher Moisture Zones". The integration of these methods proved effective in monitoring changes in the dam's physical properties, complementing traditional techniques.

Keywords: Tailings Dam; Ambient Noise Seismic Interferometry; Electrical Resistivity.

Resumo: As barragens de rejeitos de mineração e resíduos industriais requerem monitoramento constante devido ao impacto ambiental e ao risco de rompimento. No Brasil, existem 941 barragens cadastradas, sendo 340 localizadas em Minas Gerais. Para o acompanhamento da integridade dessas estruturas, são realizados monitoramentos por meio de inspeções visuais e instrumentação convencional, como piezômetros, o que demanda tempo e planejamento para o processamento dos dados. Métodos geofísicos surgem como alternativas complementares, proporcionando maior cobertura e rapidez na aquisição de dados. Assim, este trabalho tem como objetivo avaliar os parâmetros físicos da Barragem B1B4, localizada em Araxá, por meio da interferometria sísmica, que monitora a variação da velocidade da onda S (Vs), permitindo avaliar mudanças no módulo de rigidez da estrutura, e da eletrorresistividade, que identifica zonas de umidade, categorizando-as em zonas de baixa (<56 ohm.m), intermediária e alta resistividade (>371 ohm.m). Os dados de interferometria mostraram maior variação de Vs durante períodos de alta pluviosidade, sugerindo alterações nas propriedades físicas do maciço. Os dados de eletrorresistividade indicaram a presença de áreas condutivas e resistivas, fornecendo informações para identificar zonas de maior umidade. A integração desses métodos demonstrou-se eficaz para monitorar mudanças nas propriedades físicas do maciço, complementando técnicas tradicionais.

Palavras-chave: Barragens de Rejeito; Interferometria Sísmica do Ruído Ambiente; Eletrorresistividade.

Received: 24/01/2025; Accepted: 08/04/2025; Published: 26/04/2025.

1. Introduction

Many countries worldwide, whether developed or underdeveloped, depend on mining activities to sustain their economies. A considerable historical growth in global mineral production is evident. According to Leal et al. (2022), mining production in 2012 was six times higher than in 2000. Mining activities generate substantial solid waste, stored in tailings dams or waste piles. According to Olivier et al. (2017), these structures are particularly vulnerable to failures, especially tailings dams, as they are built with mining residual materials, are often heightened during operation, and frequently lack proper regulation in developing countries. These factors, combined with the high cost of post-closure maintenance, significantly increase failure risks, which are 100 times higher than those of conventional dams (Azam & Li, 2010). Hariri-Ardebili (2017) argues that probabilistic risk assessments can improve understanding of failure mechanisms and reduce uncertainties.

In dam construction engineering, geotechnical knowledge of installation sites, including stress and seismicity data, is critical for project calculations (Mendes, 2018; Silveira et al., 2021; Silveira & Pedroso, 2018). In Brazil, dams of various sizes are used for purposes such as water storage, energy generation, industrial waste retention, and mining tailings containment (Esposito et al., 2010). The design and construction of tailings dams require understanding material properties, site conditions, and risks from mining blasts or seismic events. Failures can arise from factors like poor maintenance, design flaws, regulatory non-compliance, toxic effluent accumulation, and foundation problems (Cardozo et al., 2016).

Given the disaster potential of tailings dams, identifying accident prevention measures is essential to ensure stability. Traditionally, compacted fills are stabilized by controlling the dry unit weight and water content of layers, similar to techniques used in building foundations and highways (Resende et al., 2013). Continuous monitoring, including visual inspections and conventional instrumentation, is key. However, geophysical methods have been increasingly used to enhance dam assessments (Mainali et al., 2015; Martini et al., 2016; Nikonow et al., 2019; Mollehuara-Canales et al., 2021).

Geophysical methods, as noted by Sá (2023), are effective for collecting large datasets quickly and providing broad survey coverage. Techniques like ambient noise seismic interferometry and electrical resistivity help diagnose geotechnical conditions of embankments. Seismic noise, mainly formed by surface waves, comprises microtremors (>1 Hz) and microseisms (<1 Hz) based on frequency content (Schuster, 2014; Hussain et al., 2017). Electrical resistivity, an effective tool for studying tailings, reflects subsurface variations in properties like salinity, water content, metal concentration, and pH, which influence electrical characteristics and indicate water movement (Martinez-Pagan et al., 2021; Freitas et al., 2024).

Geophysical methods are important for early warning systems, identifying subtle changes in soil stiffness and water saturation that may signal impending failure (Pankow et al., 2014). Since 2018, they have been widely implemented for monitoring mining dams in Brazil (Dias et al., 2022). Integrating geophysical techniques with conventional instrumentation improves management efficiency. For instance, seismic interferometry detects structural rigidity changes through S-wave velocity analysis, while resistivity identifies anomalies within embankments (Braga & Gama, 2024). These methods play a crucial role in detecting seepage conditions early (Mainali et al., 2015).

This study applies geophysical methods, specifically electrical resistivity and ambient noise seismic interferometry, to assess physical parameters and their correlation with geological-geotechnical conditions. The goal is not only to monitor the stability of tailings dams but also to provide insights for disaster prevention.

2. Study area

The study area lies within the Alto Paranaíba Igneous Province, part of the southern Brasília Fold Belt in the eastern Tocantins Structural Province (Almeida et al., 1977). This orogenic belt developed along the São Francisco Craton's western margin during the Neoproterozoic. It features metasediments like schists and quartzites, alongside Neocretaceous intrusive and extrusive bodies from mafic-ultramafic alkaline and ultrapotassic magmatism (Jácomo et al., 2010).

The B1B4 Dam, part of the Mining Chemical Complex of Araxá in western Minas Gerais, primarily supported phosphate extraction. Built to contain fine cyclone tailings from industrial processes, the dam began operations in 1979 and ceased in March 2019.

Initially two structures, B1 (left valley) and B4 (right valley), the dam was joined at elevation 978.00 m, forming a single mixed structure. Following the construction of both structures, the raises were carried out using the centerline method with the tailings material itself. Figure 1 depicts the dam's main components as well as a typical section showing

the embankment's main constituent materials. The dam's foundation is primarily composed of a layer of weathered rock overlain by residual soil.

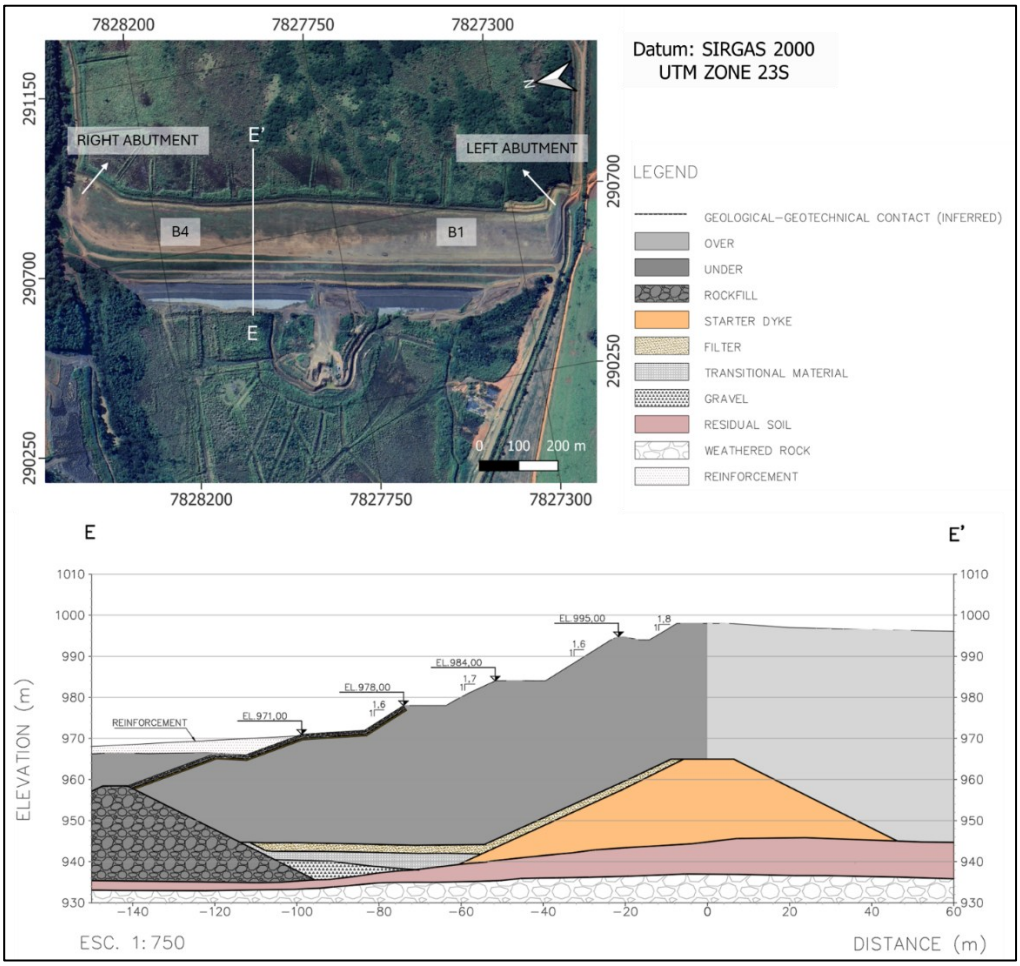

Figure 1 – Representation of the general arrangement of the dam under study. E-E' represents a typical section of the embankment. Source: Authors (2025).

3. Material and Methods

3.1. Data Acquisition

Even though the dam under study has ceased its operations, destabilization processes may occur. To identify them, conventional instrumentation (piezometers and water level indicators) is used, and to support them, geophysical monitoring systems have been installed on the dam. For geophysical monitoring, the microseismic method, including ambient noise seismic interferometry, was used to better understand the embankment's stiffness based on S-wave velocity variations. Additionally, given the wide applicability of the Electrical Resistivity (ER) method in dam investigations, it was chosen for the embankment study to enhance knowledge about the dam, especially regarding uncontrolled seepage within the embankment and abutments.

3.1.1. Ambient Noise Seismic Interferometry (ANSI)

Data acquisition using the ANSI technique involves installing a grid of sites along the structure to be monitored, such as a dam. These sites continuously record ambient seismic noise, which is generated by both human activities and natural

phenomena. The fundamental steps of seismic interferometry operation involve two stages: obtaining the cross-correlation of a pair of signals recorded from a given source and stacking the resulting cross-correlations (Curtis et al., 2006). According to Rodrigues et al. (2019), this operation can be understood as detecting the travel time difference of waves recorded between a pair of receivers.

The ANSI methodology is based on the extraction of the Green's function between two sensors. Green's function represents the wavefield recorded over time at one sensor when an impulsive source is triggered at the other sensor (Planès et al., 2016). As explained by Wapenaar et al. (2010), the term 'seismic interferometry' refers to the principle of generating new seismic responses from virtual sources by cross-correlating seismic observations at different receiver locations. Thus, the signals captured by the sites are processed through cross-correlation, allowing for the determination of the travel time of seismic waves between the sensors (Wapenaar et al., 2010). This process enables the estimation of the seismic wave propagation velocity variations in the monitored medium.

To achieve real-time data processing and the necessary sensitivity to identify small variations in propagation velocity, the most dispersive portion of the acquired wave spectrum, known as the coda wave, is utilized. The multiple scattering of this wave allows for prolonged sampling of the medium, making small velocity changes perceptible (Rodrigues et al., 2019). The propagation velocity of mechanical waves is an intrinsic property of the medium, governed by established physical laws. The velocity changes measured in the coda wave are primarily variations in the velocity of S-waves (Wit & Olivier, 2017), which are body waves associated with the shear stress of the propagation medium.

Thus, when the material is losing stiffness, there is an increase in the S-wave arrival time for a pair of sensors, indicating that the monitored medium is losing velocity. According to Breton et al. (2021), the variation in shear wave velocity (Vs) depends on the ratio between the shear modulus (μ) and the density of the medium (ρ). Additionally, it is worth noting that S-waves do not propagate in fluid media, meaning that the loss of velocity is related to this factor. In this case, the velocity of a shear body wave (Vs), which involves pure shear, is given by the equation 1:

$$Vs = \sqrt{\frac{\mu}{\rho}} \tag{1}$$

These factors are particularly important in monitoring the structure of dam embankments. In the dam under study, six geophones were installed along the embankment, with four uniaxial and two triaxial geophones, covering the dam, recording data in a 24-hour in real-time monitoring regime. Sites 1 to 6 were positioned along the dam crest, with sites 1 and 2, both triaxial, installed at each abutment. Sites 7 and 8 were installed on the slope (Figure 2). For monitoring this dam, the Trace software, developed by the Institute of Mine Seismology (IMS), was used to process and analyze the seismic records from this dam from July 2020 to February 2024.

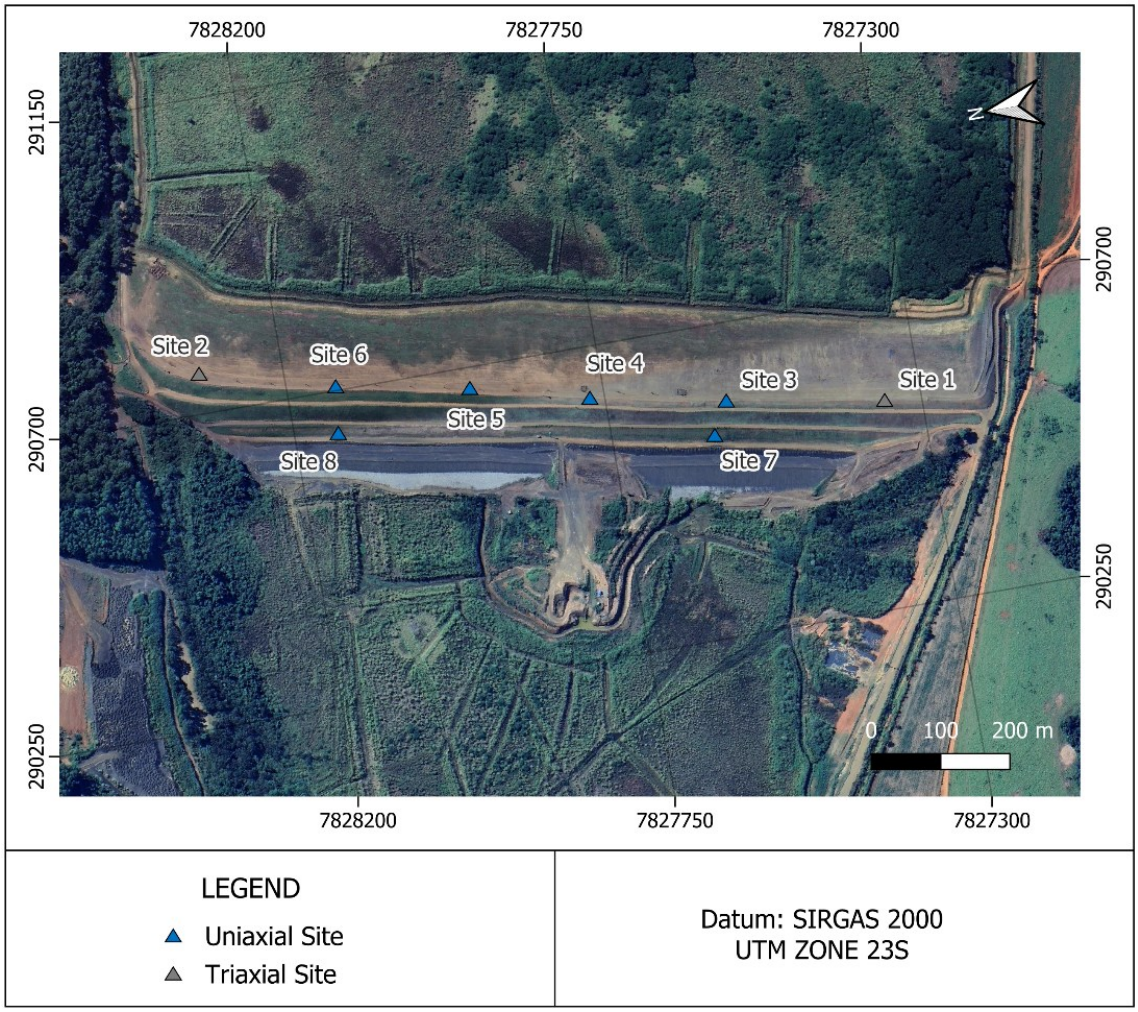

Figure 2 – Location map of the sites for microseismic monitoring.
Source: Authors (2025).

3.1.2. Electrical Resistivity (ER)

The Electrical Resistivity (ER) method involves measuring the electrical resistivity of the soil, which is influenced by the presence of water and other physical properties of the material. Data acquisition is performed by installing electrodes along the area to be investigated. These electrodes are used to inject electrical current into the ground and measure the resulting potential difference, thereby constructing an image of the electrical resistivity distribution in the subsurface. Data interpretation involves analyzing the obtained resistivity sections, where anomalies such as low resistivity zones may indicate areas with high moisture, while high resistivity zones may correspond to dry areas. This method is effective in identifying seepages, weak zones, and other anomalies that may compromise the structural safety of the dam.

The equipment used for data acquisition included the SAS 4000 resistivity meters from ABEM and the SuperSting from AGI, both configured with 64 channels and a 3.0 meter electrode spacing (L-01 to L-18). Before starting data acquisition, electrode array tests were performed. The Dipole-Dipole array demonstrated a considerably better signal-to-noise ratio at the dam under study, as well as an adequate relationship between investigation depth and lateral resolution, confirming what has already been observed in published works (Dahlin and Zhou, 2004; Loke et al., 2013; Sá et al., 2023).

The electrical resistivity campaign under analysis, conducted from July to September 2020, was the last one performed on the dam since its operations ceased in 2019. During this survey, 21 electrical resistivity sections were executed along the dam body and the beach of the B1B4 dam, totaling 16067.29 meters. Sections L-01 to L-03 were acquired in the beach

area of the embankment, oriented parallel to the structure's axis, with a line spacing of 40 meters. Sections L-04 to L-12B were collected in the dam body region, also parallel to the axis, with line spacing ranging from 15 to 30 meters. Sections L-10 to L-12 were interrupted due to a moisture area in Dam B1, which prevented their continuation. Sections L-13 to L-18 were acquired both in the beach and dam body areas, oriented perpendicular to the axis, with line spacing varying from 80 to 130 meters. Figure 3 shows the location of the ER sections in plan view, along with the topographic base of the structure.

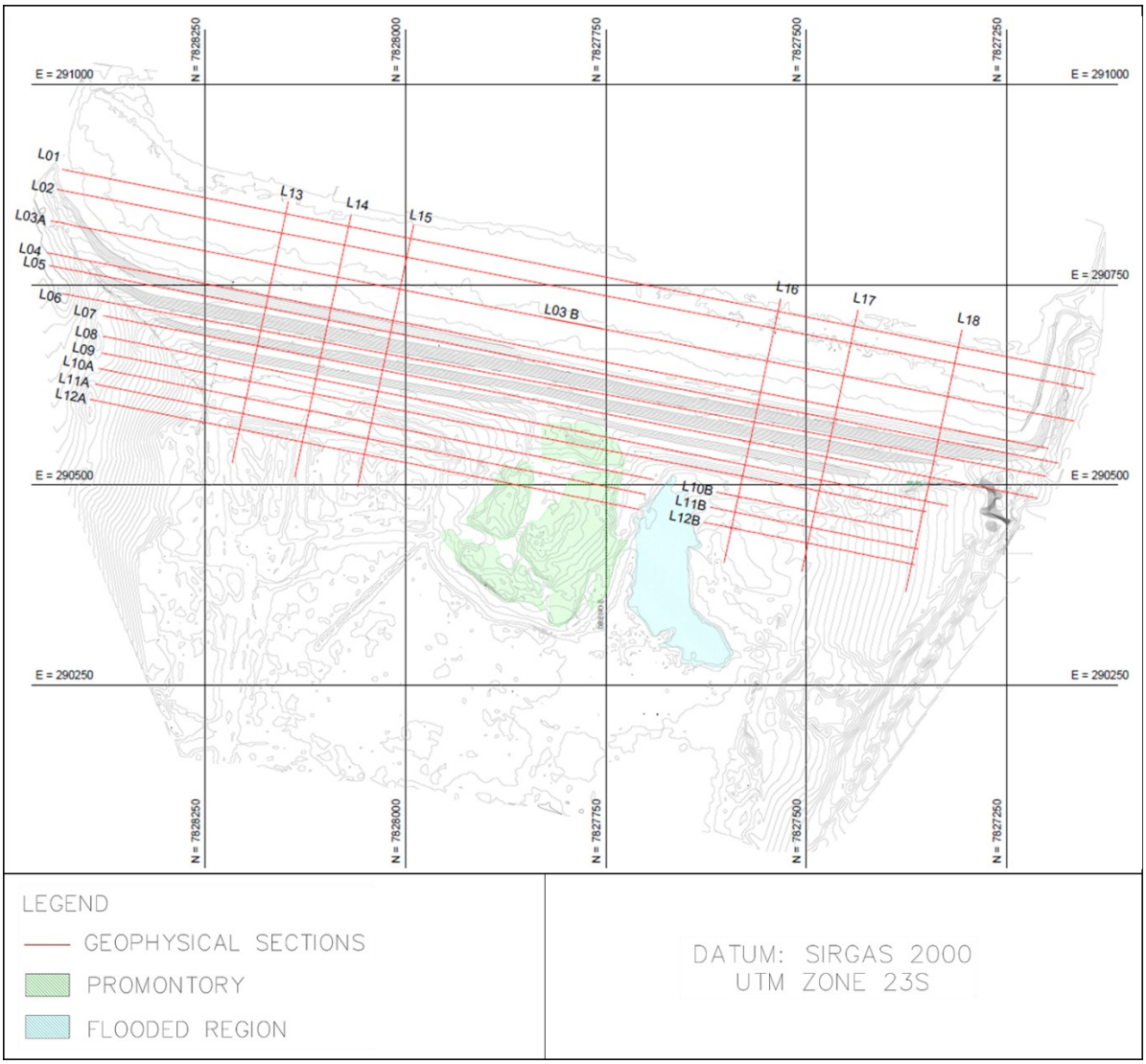

Figure 3 – Electrical resistivity survey sections at the dam. Sections L-01 to L-12 are parallel to the dam axis, and sections L-13 to L-18 are perpendicular to the axis.
Source: Authors (2025).

3.2. Data Interpretation

The interpretation of ANSI data involves some steps. Initially, the cross-correlation of seismic signals helps to calculate variations in shear wave propagation velocity, a physical property that can indicate the structural integrity of the dam. The analysis of Coda waves, the most dispersive part of the wave spectrum, increases sensitivity in detecting small velocity variations, revealing changes in the physical properties of the medium, such as the shear modulus and density. Continuous

and real-time interpretation of these data allows for the mapping of anomalies, such as high moisture zones or internal erosion, facilitating early detection of structural problems and the implementation of preventive measures, making this technique a powerful and non-invasive tool for risk management in dams. All data are extracted from the Trace software developed by the Institute of Mine Seismology (IMS), processed, and interpreted.

In this study, data from July 2020 to February 2024 were evaluated, observing variations in S-wave velocity and rainfall indices to assess the dam's stiffness.

The interpretation of the electrical resistivity data began with the processing of the raw data using the Res2DInv software. These processed data were then imported into a 3D visualization software (Leapfrog Geo), where they were integrated with the structural features of the dam and the available geotechnical information. Following this integration, each Electrical Resistivity Tomography (ERT) section was thoroughly analyzed, and the anomaly ranges were compared with water level measurements. This analysis allowed the identification of three distinct resistivity zones for each campaign: Low Resistivity Zones (LRZ), potentially indicating areas with high humidity or clay content; High Resistivity Zones (HRZ), corresponding to dry regions; and Intermediate Resistivity Zones (IRZ), which fall between these two extremes. A similar classification approach has been employed in studies of other earth dams by Camarero and Moreira (2017), as well as Sá (2023) and Oliveira (2023).

To carry out detailed modeling, the geophysical data were imported into a three-dimensional environment, generating a cloud of points with coordinates (X, Y, and Z) and their respective apparent resistivity (RES) values. The points were further classified based on their resistivity values, with points below 56 ohm.m being identified as "Zones of Higher Moisture and/or Clay Content," consistent with materials exhibiting pore moisture and/or clayey characteristics. Finally, bounding volumes were created for these categorized points using the “intrusive interpolation” option in Leapfrog. (Figure 4).

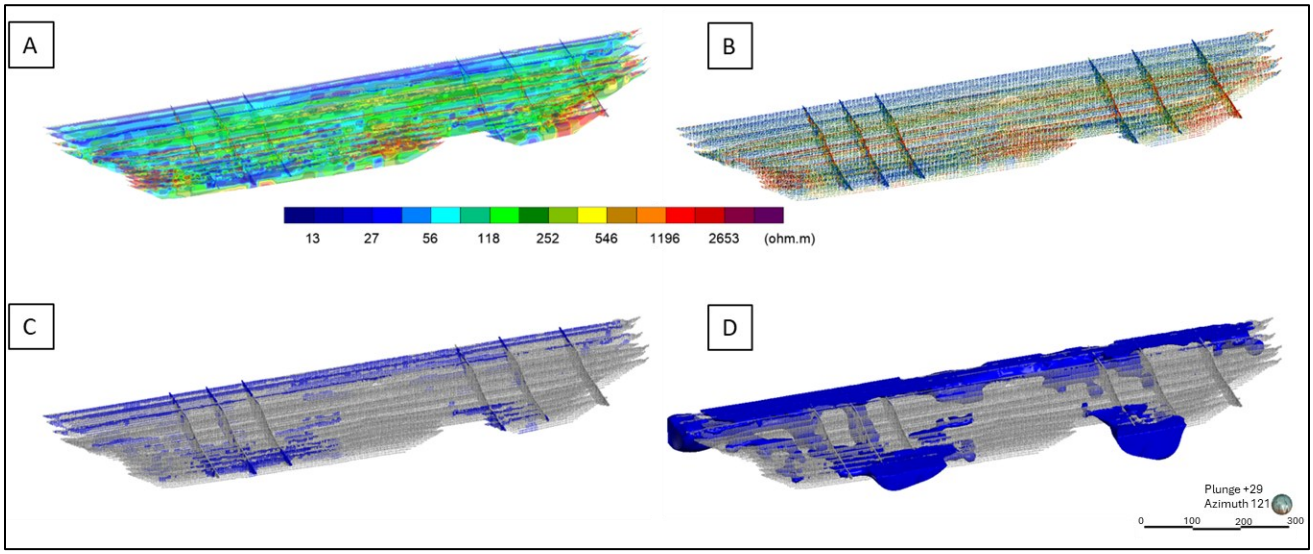

Figure 4 – A: Import of georeferenced points containing information about the apparent resistivity of materials; B: Categorization of low-resistivity points as “Moisture Zones”; C: Creation of surfaces from the categorized points; D: Generation of volumes based on the delimitation of surfaces within the dam's context.
Source: Authors (2025).

4. Results and Discussions

4.1. Ambient Noise Seismic Interferometry

The ANSI data were processed using the trace software, resulting in the graph shown in Figure 5. Overall, the graph indicates the variation in S-wave velocity in relation to rainfall indices. During the analysis period (July 2020 to February 2024), some sites presented issues, represented by a continuous line on the graph. However, this did not interfere with the overall data analysis.

The results indicate, in general, an increase in S-wave velocity (Vs) between July and October 2020, a period characterized by little or no rainfall. However, between July and September, a slight decrease in Vs velocity (%) is observed, as shown at the beginning of the graph. Between October 2020 and February 2021, which was generally a rainy period, the S-wave velocity showed some variations but exhibited a consistent decline, reaching a minimum of -1%, representing a total drop of 5%. During this period, on some days in November 2020, the precipitation level reached 5 mm, causing an increase in S-wave velocity (Vs). However, shortly after, precipitation levels rose to around 80 mm, leading to a further decrease in Vs. Between January and February 2021, there was a recovery in velocity of approximately 1%, as there was no rainfall during this time. However, the velocity began to drop again after consecutive rainy days, with precipitation levels ranging between 82 and 10 mm.

Subsequently, after the rainy period, the sites recorded an increase in S-wave velocity of around 4% until October 2021. However, some variations in this velocity were observed due to isolated rainfall events, with precipitation levels of up to 20 mm. Despite this, the recorded rainfall volume was not sufficient to cause a significant reduction in S-wave velocity. However, one of the sites did not show the same velocity gain as the others.

Between October 2021 and February 2022, the sites showed a general decreasing trend of 4%, with variations ranging from 2% to 4% depending on the precipitation levels. For example, between December and February, rainfall reached around 110 mm. During this period, the sites recorded more significant velocity decreases (approximately 2.5%). However, between October and November, when precipitation was around 70 mm, the sites showed a smaller decrease in S-wave velocity (Vs) of approximately 1.5%.

After this period, there was an interval with an S-wave velocity gain of around 4.2% until October 2022, with some minor decreases of around 0.5% due to isolated rainy days. During this time, rainfall peaked at 40 mm, with an average of 10 mm. From October 2022 to February 2023, the sites showed an overall velocity decrease of 2.5%, coinciding with most rainy days during this period. However, between October and November, precipitation levels varied between 0 and 25 mm, and Vs showed almost no variation. However, when precipitation reached 80 mm, Vs began to decrease, a trend that extended until February.

Following this period, the velocities recorded by the sites showed little variation, with gains of approximately 1.5% until November 2023, as this was a period with low precipitation levels. From November 2023 to February 2024, the sites exhibited a decrease in S-wave velocity of about 0.5%, coinciding with the start of the rainy season, which presented precipitation levels higher than those of the previous period. It is worth noting that from February 2023 to February 2024, in general, the Vs values showed almost no variation, which may be associated with a loss of geophone signal during this period. It is worth noting that even during rainy periods, on days with lower precipitation, the S-wave velocity (%) does not decrease as much as on days with higher rainfall (mm).

According to Olivier et al. (2017), changes in seismic velocity in tailings dams are driven by variations in stress within the medium, saturation levels, physical impacts on the dam body, and pore pressure changes.

As noted by Breton et al. (2021), an increase in the arrival time of S-waves between a pair of sensors indicates a reduction in wave velocity within the monitored medium, which suggests that the material may be losing stiffness.

In this context, the results obtained demonstrate a clear correlation between the reduction in S-wave propagation velocity and increased rainfall. The most significant velocity decreases were observed between October and February, which correspond to the months with the highest rainfall levels in the region where the dam is located. This relationship highlights how increased rainfall likely leads to elevated saturation levels in the dam body, altering its mechanical properties and reducing its stiffness. It is important to note that variations in velocity may be influenced by additional factors and are not solely dependent on rainfall levels. These other factors could include changes in stress distribution, temperature variations, or localized material heterogeneities, which may also contribute to the observed velocity patterns.

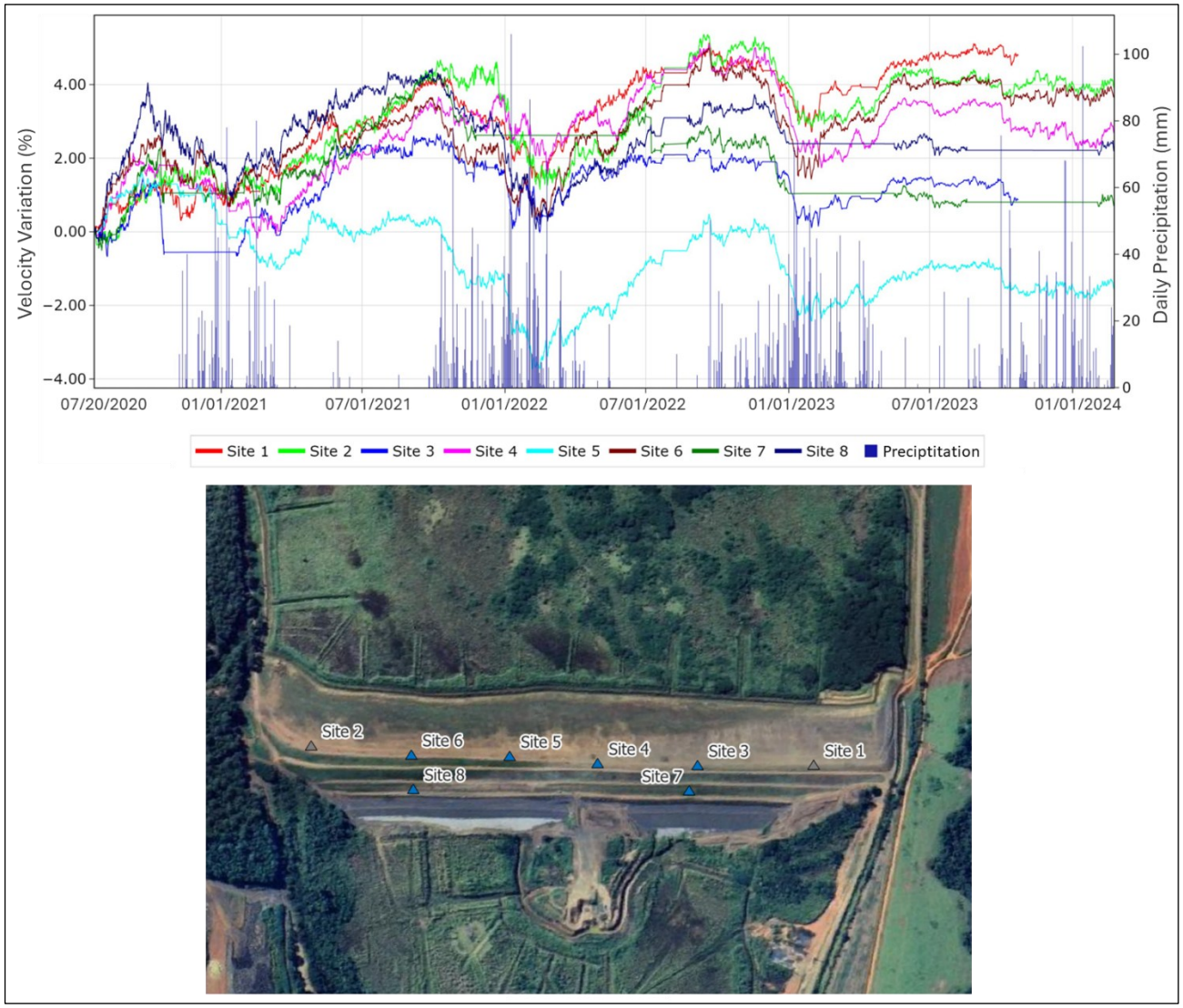

Figure 5 – History of velocity variations recorded by each sensor in the monitoring system from July 2020 to February 2024. Sensors 1 and 2 are triaxial, while sensors 3 to 8 are uniaxial.
Source: Authors (2025).

4.2. Eletrical Resistivity (ER)

The electrical resistivity profiles allowed the investigations down to depths of approximately 50 meters. The collected data reliably differentiated between high, low, and intermediate resistivity anomalies, which were categorized according to their magnitude (Figure 6). High Resistivity Zones (HRZ), with values above 371 ohm.m, were interpreted as dry zones, while Low Resistivity Zones (LRZ), with values below approximately 56 ohm.m, were correlated with regions of high humidity. Intermediate Resistivity Zones (IRZ) represented areas with resistivity values falling between these limits.

Sections L-01 to L-03, located in the tailings beach area, exhibited low resistivity values, indicating an environment with higher moisture content. The presence of low-resistivity zones in this region suggests that water accumulation in the tailings beach may impact the near-surface layers.

Sections L-04 to L-09, situated in the dam body region, showed a lower predominance of low apparent resistivity values. In the surface layers, a higher concentration of intermediate to high resistivity values was observed, distributed

continuously. Just below, conductive zones extend deeper, forming subvertical patterns. At greater depths, a gradual increase in resistivity occurs, with noticeable variations between zones of different geophysical characteristics.

Sections L-10A, L-11A, L-12A, L-10B, L-11B, and L-12B, located along the dissipation basin of the dam, exhibit similar geophysical characteristics. The initial sections ("A") display a subsurface horizon with resistivity ranging from conductive to intermediate, followed by a highly conductive zone that gradually increases in resistivity with depth. In the "B" sections, a predominance of low resistivity values is observed from the surface layers to greater depths, with a sharp transition to highly resistive zones from the central portion to the end of the profiles.

Sections L-13 to L-18, arranged perpendicular to the dam axis, presented a conductive surface horizon extending deeper in the initial parts of the profiles. Localized resistive anomalies appear within this layer in some sections. The central region is characterized by a resistive subsurface layer overlying a discontinuous conductive zone, which becomes more resistive at greater depths. In the final portions of the profiles, near the downstream side of the dam, low resistivity values predominate, except for section L-18, which exhibits high resistivity values throughout the final stretch.

Based on the acquired geophysical data (Electrical Resistivity – ER) and their corresponding signatures in the context of the existing structures of the dam, it became possible to identify the probable materials present in the area and discuss their possible moisture conditions.

After defining the characteristic resistivity values for the Low Resistivity Zones (LRZ), implicit modeling of the "Zones of Higher Moisture" was performed. These zones correspond to areas with a higher concentration of low apparent resistivity values, characterized by greater persistence and continuity between adjacent geophysical sections, indicating the potential presence of pore moisture and/or clay content. The distribution, shape, and continuity of the conductive anomalies were essential for defining the range associated with these "Higher Moisture Zones", which was determined to be between 0 and 41 ohm.m.

The regions with resistivity between 0 and 41 ohm·m were identified in the tailings beach area, showing lateral continuity along the dam axis and greater depth in the region of B4 Dam, reaching approximately 45 m. Near the intersection with the right abutment of the same dam, there is an area with depths ranging from 10 m to 15 m. Another area within B4 Dam reaches depths of 28 m to 33 m at the crest, extending downstream. A third region, also within B4 Dam, has a maximum depth of 45 m at the crest and variations between 11 m and 17 m near the toe drain. Additionally, anomalies were identified downstream of both B4 and B1 dams, with the one downstream of B1 being observed in the field.

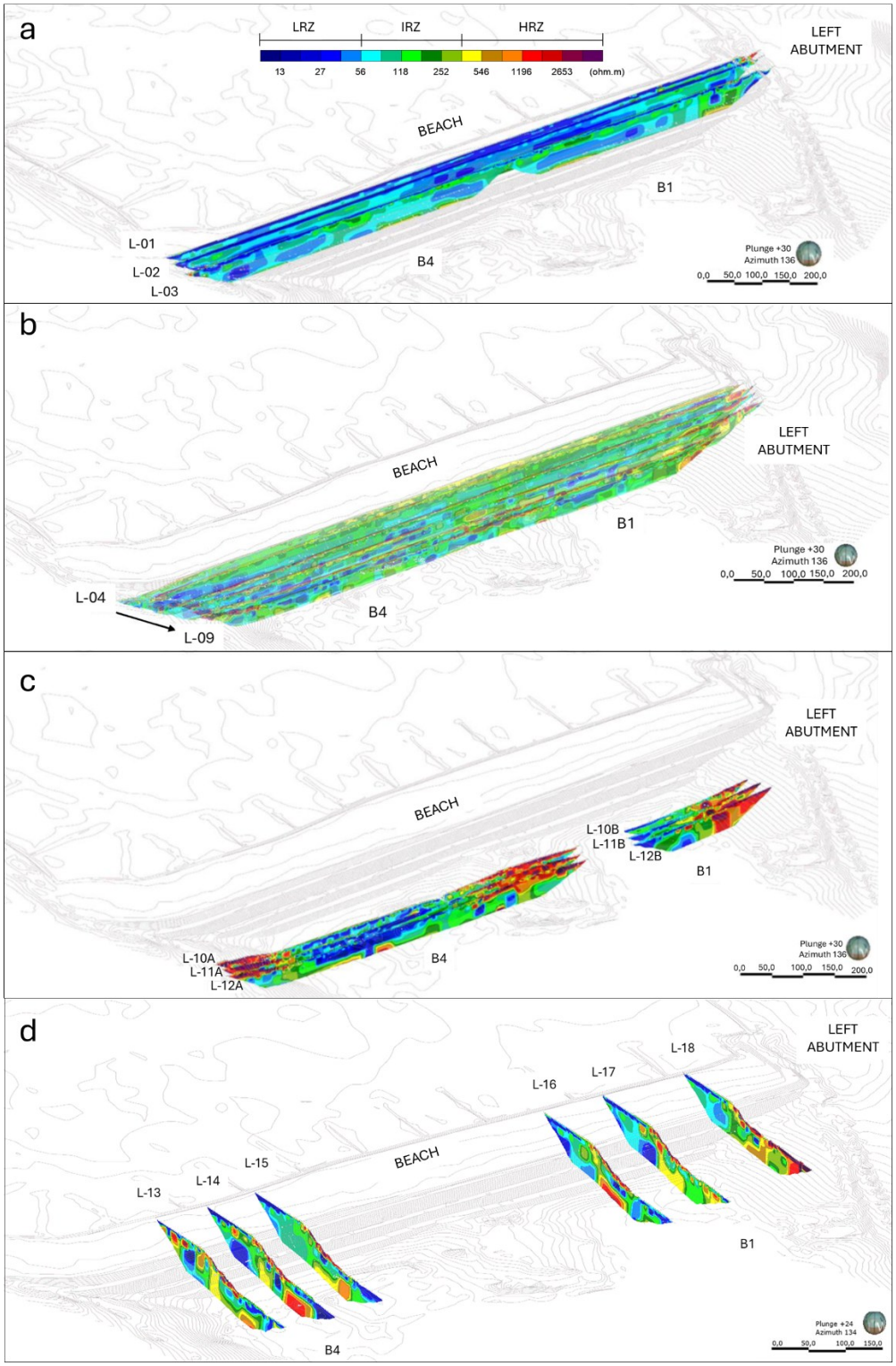

Figura 6 – Representation of the acquired electrical resistivity sections. a) L-01 to L-03 section b)L-04 to L-09 section c)L-10A to L-12B section d) L-13 to L-18 section.
Source: Authors (2025).

Figure 7 illustrates the "Higher Moisture Zones" modeled in the context of the main dam structures, such as the starter dyke and the toe drain. The analysis reveals that the toe drains, drainage blanket, and the overlying regions of B1B4 Dam are located in conductive areas (LRZ), likely associated with local moisture. This behavior is corroborated by field observations, in which a higher concentration of water in the downstream region of the dam body coincides with the zones of higher conductivity identified in the Electrical Resistivity (ER) sections.

Beneath the toe drain, in the foundation, there is a noticeable trend of increasing resistivity values (greater than 118 ohm.m), with continuous morphological characteristics observed in several sections. This geophysical pattern is visible at the base of the drainage structure and provides a clear signature of this transition. Below these areas, an increase in apparent resistivity values (greater than 118 ohm.m) can again be observed, likely associated with the foundation material, where moisture levels are lower (Figure 8).

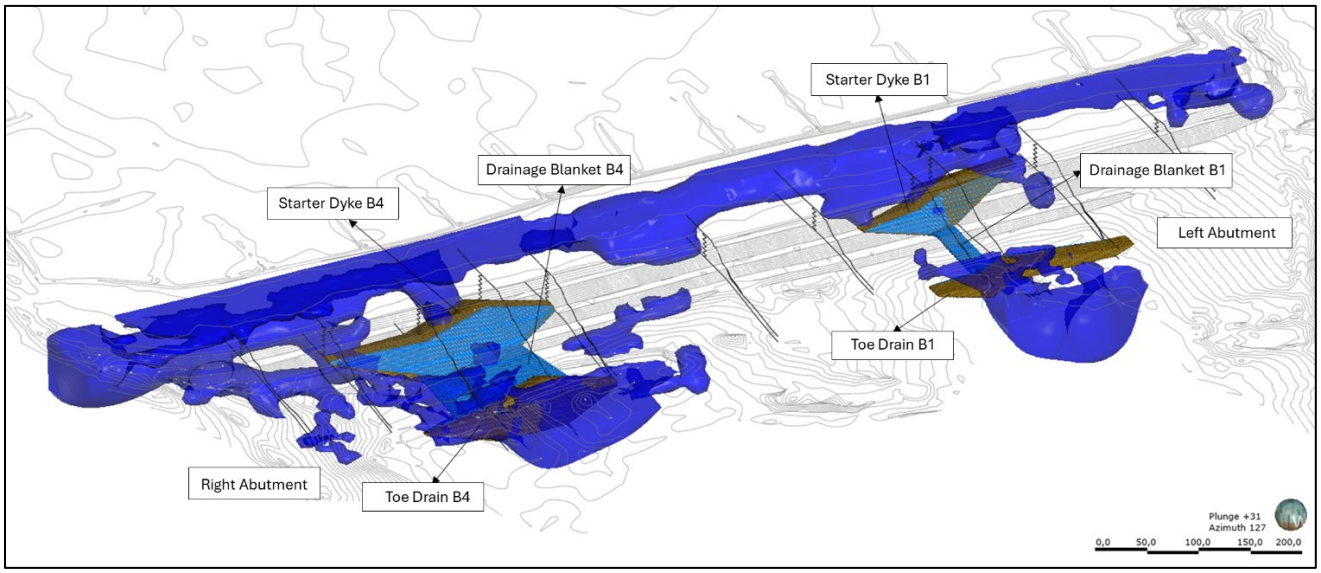

Figure 7 – Representation of the "Higher Moisture Zones" in the context of B1B4 Dam, based on geophysical electrical resistivity data, correlated with the dam's main structures, including the starter dyke, toe drains and drainage blanket. Source: Authors (2025).

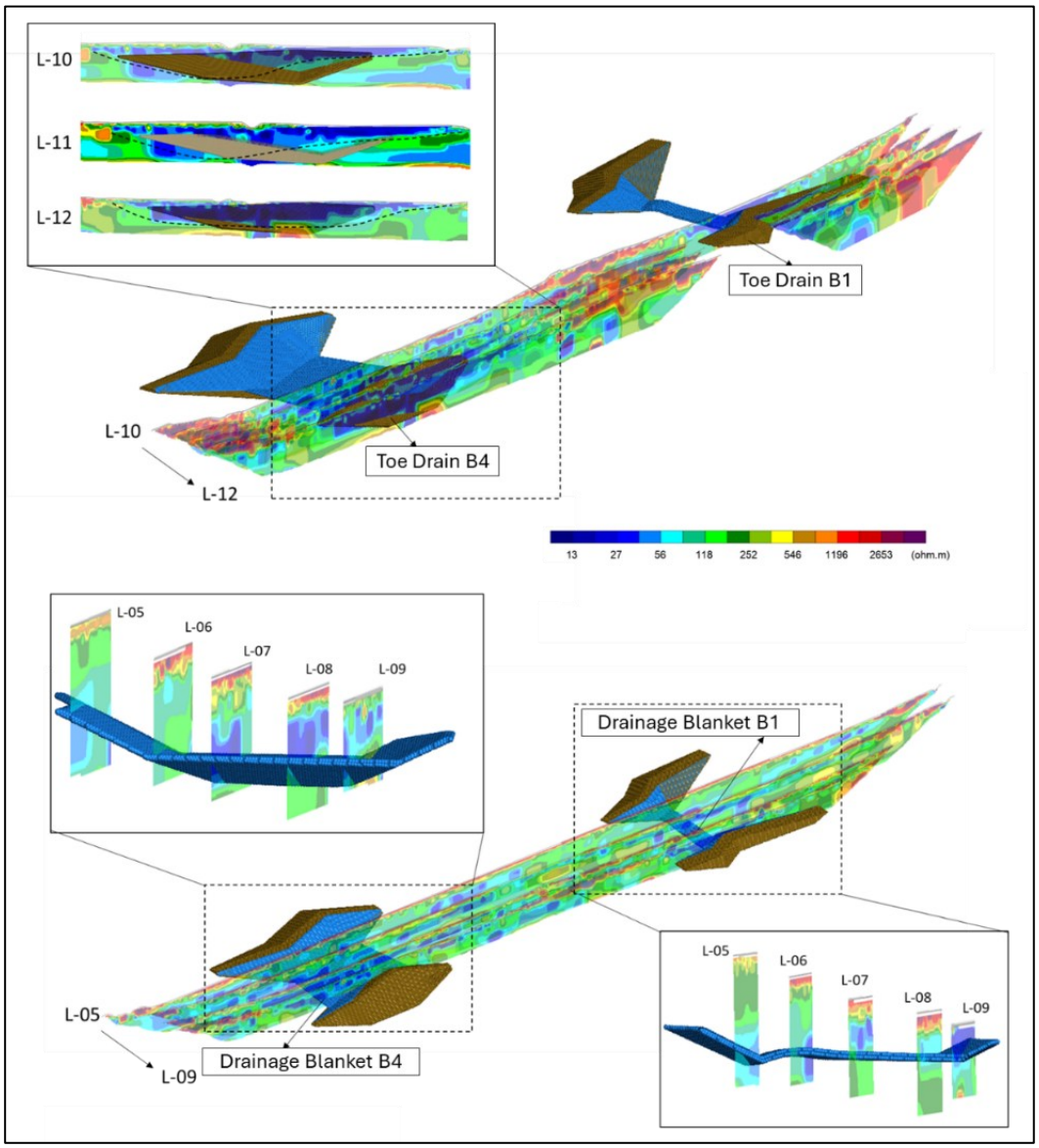

Figure 8 – Characterization of materials from the toe drain and drainage blanket of the B1B4 Dam and correlation with geoelectrical signatures. Source: Authors (2025).

It was observed that the reduction in S-wave velocity (Vs) detected during the ANSI monitoring, between July and September 2020, could possibly be associated with areas identified as having high conductivity in the electrical resistivity profiles. These areas, located in the toe drains, drainage blanket, and tailings beach, align with the "Zones of Higher Moisture" modeled based on low resistivity values (<56 ohm.m) from the Electrical Resistivity (ER) data. The observed decrease in S-wave velocity is consistent with the reduced stiffness of materials in regions with elevated pore moisture and/or clay content, as indicated by the conductive anomalies.

The correlation between both methods underscores the relationship between mechanical properties and geophysical signatures of the dam materials. The conductive zones identified by the ER method not only validated the moisture distribution inferred from the seismic velocity variations but also provided a detailed spatial characterization of these areas, highlighting their continuity and connection to the structural features of the dam. These findings demonstrate the complementary nature of the two methods, where resistivity measurements offer precise localization and classification of

moisture zones, while seismic interferometry provides dynamic insights into the mechanical changes within the dam body over time.

5. Final remarks

During the analyzed period, the ambient noise seismic interferometry data indicated a cyclic trend in the variations of S-wave velocity (%). Between October and February, when precipitation levels are higher, the Vs shows more pronounced decreases. On the other hand, between February and October, characterized by lower precipitation levels, a recovery in Vs is observed, suggesting a gain in rigidity in the dam. Moreover, it was observed that the inflection in S-wave velocity (Vs) at the beginning of microseismic monitoring in July to September, could be related to high-conductivity areas identified in the toe drains, drainage blanket, and the tailings beach through electrical resistivity measurements.

The correlation between low resistivity and low S-wave velocity (Vs) proved essential for identifying atypical regions within the dam, such as areas with higher moisture content. By integrating seismic interferometry data from ambient noise with electrical resistivity measurements, a comprehensive approach was achieved for monitoring variations in the dam's physical properties.

This study reinforces the importance of continuous geophysical monitoring as a complementary tool to conventional instrumentation, contributing to the preventive assessment of the dam and the management of associated geotechnical risks.

References

ALMEIDA, F. D.; HASUI, Y.; BRITO NEVES; B. D.; FUCK, R. A. Províncias estruturais brasileiras. In: *Simpósio de Geologia do Nordeste*, 1977, Campina Grande, v. 8, p. 363-391, 1977.

AZAM, S., LI, Q. Tailings Dam Failures: A review of the last one hundred years. *Geotechnical News*, v. 28, n. 4, p. 50–54, 2010.

BRAGA, M.A.; GAMA, M.F. Advancements in geophysical monitoring of tailings dams: Integrating geophysical methods with geotechnical instrumentation for improved safety and environmental management. In: *International Workshop on Gravity, Electrical & Magnetic Methods and Their Applications, Shenzhen, China*. Society of Exploration Geophysicists and Chinese Geophysical Society, p. 7-10, 2024.

BRETON, M. L.; BONTEMPS, N.; GUILLEMOT, A.; BAILLET, L.; LAROSE, É. Landslide monitoring using seismic ambient noise correlation: challenges and applications. *Earth-Science Reviews*, v. 216, p. 103518, 2021.

CAMARERO, P.L.; MOREIRA, C.A. Geophysical investigation of earth dam using the electrical tomography resistivity technique. *REM-International Engineering Journal*, v. 70, p. 47-52, 2017.

CARDOZO, F. A. C.; PIMENTA, M. M.; ZINGANO, A. C. Métodos construtivos de barragens de rejeitos de mineração – uma revisão. *Holos*, v. 8, n. 32, p. 77-85, 2016.

CURTIS, A.; GERSTOFT, P.; SATO, H.; SNIEDER, R.; WAPENAAR, K. Seismic Interferometry-turning noise into signal. *The Leading Edge*, v. 25, n. 9, p. 1082–1092, 2006.

DAHLIN, T.; ZHOU, B. A numerical comparison of 2D resistivity imaging with 10 electrode arrays. *Geophysical Prospecting*, v. 52, n. 5, p. 379-398, 2004.

DIAS, L. S. O.; BRAGA, M. A.; CUNHA, A. S.; OLIVIER, G.; MACHADO, D.M. 2022. Mining Induced Ground Motions in a Tailings Dam. *Anuário do Instituto de Geociências*, v. 45, p. 1-12, 2022.

ESPÓSITO, T.J.; DUARTE, A. P. Classificação de barragens de contenção de rejeitos de mineração e de resíduos industriais em relação a fatores de risco. *Rem: Revista da Escola de Minas*, v. 63, n. 2, p. 287-295, 2010.

FREITAS, I. V. L. D.; SANTOS, H. A. E. The relationship between geophysical and geotechnical data: a temporal analysis of an iron ore tailings dam. *Soils and Rocks*, v. 47, n. 4, p. e2024011923, 2024.

HARIRI-ARDEBILI, M. A. Risk, Reliability, Resilience (R3) and beyond in dam engineering: A state-of-the-art review. *International Journal of Disaster Risk Reduction*, v. 31, p. 806-831, 2018.

HUSSAIN, Y.; MARTINEZ-CARVAJAL, H.; CÁRDENAS-SOTO, M.; UAGODA, R.; MARTINO, S.; HUSSAIN, M. B. Microtremor response of a mass movement in Federal District of Brazil. *Anuário do Instituto de Geociências*, v. 40, n. 3, p. 212-221, 2017.

JÁCOMO, M. H.; BROD, T. C. J.; PIRESA, A. C. B.; BRODA, J. A., PALMIERIC, M.; FERRAR, A. J. D. Associação de magnetometria, gamaespectrometria, geoquímica e petrografia para modelamento tridimensional da mineralização de nióbio do depósito Morro do Padre, Goiás, Brasil. In: *IV Simpósio Brasileiro de Geofísica*. European Association of Geoscientists & Engineers, p. cp-197-00061, 2010.

LEAL, F.C.A.; GOMES, W.V.G.; SILVA, P.J.L.; GONÇALVES, P.H.F.; NETO, O.F.; JÚNIOR, O.F.S. Uma revisão dos acidentes em barragens de rejeito de mineração da América do Sul e o cenário brasileiro. *Revista de Geociências do Nordeste*, v. 8, n. 1, p. 10-27, 2022.

LOKE, M.H.; CHAMBERS, J.E.; RUCKER, D.F.; KURAS, O.; WILKINSON, P.B. Recent developments in the direct-current geoelectrical imaging method. *Journal of Applied Geophysics*, v. 95, p. 135-156, 2013.

MAINALI, G.; NORDLUND, E.; KNUTSSON, S.; THUNEHED, H. Tailings dams monitoring in Swedish mines using self-potential and electrical resistivity methods. *Electronic Journal of Geotechnical Engineering*, v. 20, n. 13, p. 5859-5875, 2015.

MARTINEZ-PAGAN, P.; GÓMEZ-ORTIZ, D.; MARTÍN-CRESPO, T.; MARTÍN-VELÁZQUEZ, S.; MARTINEZ-SEGURA, M. Electrical resistivity imaging applied to tailings ponds: an overview. *Mine Water and the Environment*, v. 40, n. 1, p. 285-297, 2021.

MARTINI, R.J.; CAETANO, T.R.; SANTOS, H.A.; ARANHA, P.R.A. Deposição de rejeitos de minério de ferro em reservatórios: uma aplicação do método GPR. *Revista Ambiente & Água*, v. 11, n. 4, p. 878-890, 2016.

MENDES, N. B. Um estudo de propagação de ondas e lançamento do sismo na análise dinâmica acoplada barragem em arco -reservatório -fundação. 289 p. Tese (Doutorado em Estruturas e Construção Civil) — Universidade de Brasília, Brasília, 2018.

MOLLEHUARA-CANALES, R.; KOZLOVSKAYA, E.; LUNKKA, J. P.; MOISIO, K.; PEDRETTI, D..Non-invasive geophysical imaging and facies analysis in mining tailings. *Journal of Applied Geophysics*, v. 192, p. 104402, 2021.

NIKONOW, W.; RAMMLMAIR, D.; FURCHE, M. A multidisciplinary approach considering geochemical reorganization and internal structure of tailings impoundments for metal exploration. *Applied geochemistry*, v. 104, p. 51-59, 2019.

OLIVEIRA, L. A.; BRAGA, M. A.; PROSDOCIMI, G.; DE SOUZA CUNHA, A.; SANTANA, L., & DA GAMA, F. Improving tailings dam risk management by 3D characterization from resistivity tomography technique: Case study in São Paulo–Brazil. *Journal of Applied Geophysics*, v. 210, p. 104924, 2023.

OLIVIER, G.; BRENGUIER, F.; WIT, T.; LYNCH, R. Monitoring the stability of tailings dam walls with ambient seismic noise. *The Leading Edge*, v. 36, n. 4, p. 9, 2017.

PANKOW, K.L.; MOORE, J.R.; HALE, J.M.; KOPER, K.D.; KUBACKI, T.; WHIDDEN, K.M.; MCCARTER, M.K. Massive landslide at Utah copper mine generates wealth of geophysical data. *Gsa Today*, v. 24, n. 1, p. 4-9, 2014.

PLANÈS, T., MOONEY, M. A., RITTGERS, J. B. R., PAREKH, M. L., BEHM, M., & SNIEDER, R. Time-lapse Monitoring of Internal Erosion in Earthen Dams and Levees Using Ambient Seismic Noise. *Géotechnique*, v. 66, n. 4, p. 301–312, 2016.

RESENDE, LINCOLN RIBEIRO MAIA DE; OLIVEIRA FILHO, WALDYR LOPES DE; NOGUEIRA, CHRISTIANNE DE LYRA. Use of the DCP test for compaction control of staged dikes in mining tailings dams. *Rem: Revista da Escola de Minas*, v. 66, n. 4, p. 493-498, 2013.

RODRIGUES, C. T.; DE PAULA, A. Q.; CORRÊA, T. R.; SEBASTIÃO, C. S.; COSTA, O. V.; MAGALHÃES, G. G.; SANTANA, L. D. Passive Seismic Interferometry's State-of-the-art–a Literature Review. Sustainable and Safe Dams Around the World/Un Monde de Barrages *Durables et Sécuritaires*, p. 2951-2960, 2019.

SÁ. G.; BRAGA, M. A.; ALMEIDA, L. A. P. E.; DIAS, L. S. D. O.; CUNHA, A. D.A.; ROCHA. D. C. G D. Geophysical Key Indicator for Tailings Dam Physical Integrity Monitoring – Brazil. *REM – International Engineering Journal*, Ouro Preto -MG, v. 76, n. 4, p. 363-370, 2023.

SCHUSTER, G. T. Seismic Interferometry. In: *Encyclopedia of Exploration Geophysics*. Society of Exploration Geophysicists, 2014. p. Q1–1–Q1–41 doi:10.1190/1.9781560803027.entry5

SILVEIRA, I. V. DA; PEDROSO, L. J. Analysis of natural frequencies and modes of vibration involving interaction dam-reservoir-foundation for concrete gravity dams. In: *Third International Dam World Conference*, p. 11, 2018.

SILVEIRA, I. V. DA; PEDROSO, L. J.; MAROTTA, G. S. Study of the influence of the foundation and the reservoir on the dynamic response in a concrete gravity dam profile. *Revista IBRACON de Estruturas e Materiais*, v. 14, n. 4, p. e14403, 2021.

WAPENAAR, K.; DRAGANOV, D.; SNIEDER, R.; CAMPMAN, X.; VERDEL, A. Tutorial on seismic interferometry: Part 1 — Basic principles and applications. Geophysics, v. 75, n. 5, p. 75A195–75A209, 2010.